areas including the anterior cingulate cortex, dorsolateral prefrontal cortex, orbitofrontal cortex, precuneus, and inferior frontal gyrus. **Conclusions:** The controls exhibited enhanced activity in brain areas involved in inhibitory control, while the AD group had hypoactivation. This is in line with the behavioural data (greater Stroop interference and more errors), suggesting altered inhibitory control in AD. Extending future studies to include mild cognitive impairment will allow for investigation of inhibitory control early on in the disease process.

P3-283 FUNCTIONAL CONNECTIVITY WITH ANTERIOR TEMPORAL LOBE REGIONS ORDERED ACCORDING TO THE BRAAK PROGRESSION SCHEME REVEALS SEQUENTIAL COUPLING TO DEFAULT MODE AND THEN SENSORY NETWORKS

Adam J. Schwarz[1], Brian A. Gordon[2], Aaron Tanenbaum[3], John C. Morris[3,4], Tammie LS. Benzinger[4,5], Beau Ances[4,6], *[1]Eli Lilly and Company, Indianapolis, IN, USA; [2]Washington University School of Medicine, St. Louis, MO, USA; [3]Washington University in St. Louis, St. Louis, MO, USA; [4]Knight Alzheimer's Disease Research Center, St. Louis, MO, USA; [5]Washington University in St. Louis School of Medicine, St. Louis, MO, USA; [6]Washington University School of Medicine, St. Louis, MO, USA. Contact e-mail: schwarz_adam_james@lilly.com*

Background: The stereotypical picture of tau spreading in the Alzheimer's brain is encapsulated in the Braak staging scheme, which posits a medial to lateral progression of tau pathology around the anterior temporal lobe that parallels a subsequent spreading of tau to the wider neocortex. Association cortices are affected before primary sensory areas. This spreading is thought to occur via distributed functional networks. We sought to understand the whole-brain functional connectivity relationships with respect to Braak staging regions in the anterior temporal lobe, to elucidate the a possible sequence of involvement of wider neocortical brain networks associated with the prototypical scheme of tau progression. **Methods:** Regions of interest were defined corresponding to the anterior temporal lobe regions specified in the simplified Braak staging procedure [1,2]. To profile the connectivity of these regions in the absence of overt Alzheimer's pathology, we examined a cohort of older cognitively normal subjects (CDR=0, N= 126, Age 45-88) and a cohort of young healthy male volunteers (N=16). Whole-brain, seed-based connectivity profiles, and contrasts in connectivity between different Braak regions, were computed. **Results:** In both groups, as the seed was moved from medial (entorhinal cortex) to lateral (superior temporal gyrus (STG)), connectivity with the default mode network (DMN) first increased (reaching a maximum at the middle temporal gyrus (MTG)) but then sharply decreased at the STG. In contrast, connectivity with the sensorimotor network (SMN) increased sharply with respect to the STG relative to the MTG (Figure). Contrast maps between connectivity patterns illustrate this selective increased and decreased connectivity with the DMN (Figure). Patterns in both groups were similar, except the younger subjects showed strong DMN correlations with the inferior temporal gyrus as well as the MTG. **Conclusions:** Considering the anterior temporal Braak regions as representing a temporal ordering from medial to lateral, the observed dependence of functional connectivity is consistent with regions such as the precuneus exhibiting tau pathology before primary sensory areas. Future work will consider how this connectivity is modified by the presence of tau pathology. [1] Braak H et al. 2006 Acta Neuropathol 112(4): 389-404. [2] Schwarz AJ et al. 2016 Brain (in press).

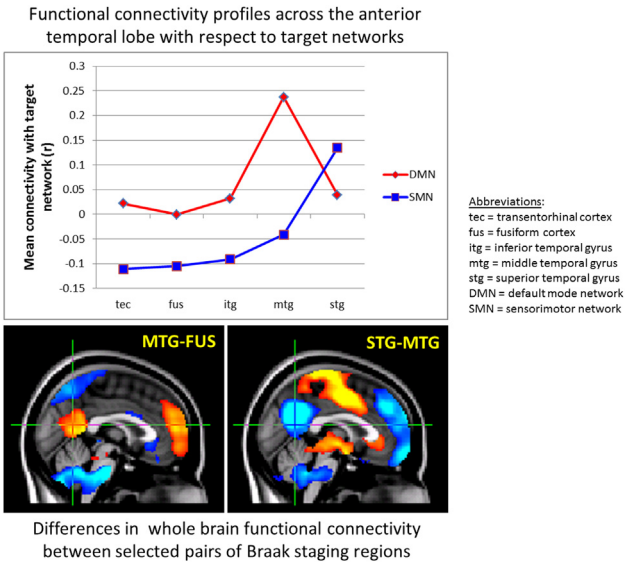

P3-284 LOWER CARDIAC INDEX LEVELS RELATE TO REDUCED CEREBRAL BLOOD FLOW VALUES IN OLDER ADULTS WITH NORMAL COGNITION AND MILD COGNITIVE IMPAIRMENT: THE VANDERBILT MEMORY AND AGING PROJECT

Angela L. Jefferson[1], Dandan Liu[1], Deepak Gupta[2], Kimberly R. Pechman[1], Susan Bell[1], Katherine A. Gifford[1], Timothy J. Hohman[1], Manus Donahue[3], *[1]Vanderbilt University School of Medicine, Nashville, TN, USA; [2]Vanderbilt University, Nashville, TN, USA; [3]Vanderbilt University Institute of Imaging Science, Nashville, TN, USA. Contact e-mail: angela.jefferson@vanderbilt.edu*

Background: Mechanisms underlying reported associations between lower cardiac index and smaller brain volume, increased white matter hyperintensities, worse cognitive performance and incident dementia are not well understood. We hypothesized that lower systemic cardiac index is associated with lower cerebral blood flow (CBF) among older adults without dementia. **Methods:** Participants with normal cognition and mild cognitive impairment (n=318, 73±7, 59% male) were drawn from the Vanderbilt Memory & Aging Project, a case control longitudinal study. Cardiac index ((stroke volume x heart rate)/body surface area, L/min/m^2) was quantified from echocardiography. CBF, the rate of blood delivery to tissue (mL blood/100g tissue/min), was assessed with pseudo-continuous arterial spin labeling MRI. Linear regression models with ordinary least square estimates related cardiac index to CBF regions of interest (ROIs) determined by multi-atlas segmentation adjusting for Framingham Stroke Risk Profile (including age, sex, systolic blood pressure, anti-hypertensive medication usage, diabetes, left ventricular hypertrophy, atrial fibrillation, and prevalent cardiovascular disease (CVD)), race, education, cognitive diagnosis, apolipoprotein E4 status, and corresponding ROI tissue volume. **Results:** Lower cardiac index levels related to lower CBF values in the temporal lobe and prefrontal cortex but not in the occipital or parietal lobes. Specifically, lower

cardiac index was associated with lower CBF in right and left hippocampi ($p<0.004$), right parahippocampal gyrus ($p=0.002$), right and left superior temporal gyri ($p<0.01$), right and left medial temporal gyri ($p<0.001$), right and left inferior temporal gyri ($p<0.004$), right and left fusiform gyri ($p<0.01$), right and left anterior cingulate gyri ($p<0.002$), right and left medial frontal cortex ($p<0.0004$), and right and left inferior frontal gyri ($p<0.006$). When models were repeated excluding participants with prevalent CVD and atrial fibrillation, findings were not attenuated. **Conclusions:** Among older adults free of dementia, systemic hemodynamics may affect cerebral hemodynamics in a regionally specific pattern independent of concurrent vascular risk factors (e.g., hypertension, diabetes) and prevalent CVD. Such compromises in cerebral circulation control may contribute to amyloid aggregation or clearance, neuronal injury, and cerebrovascular damage. Further investigation into the mechanisms linking cardiac index, regional CBF, and corresponding brain health consequences is merited. Funding: IIRG-08-88733, R01-AG034962, K24-AG046373, UL1-TR000445, K23- AG045966, K23-AG048347, K12-HD043483.

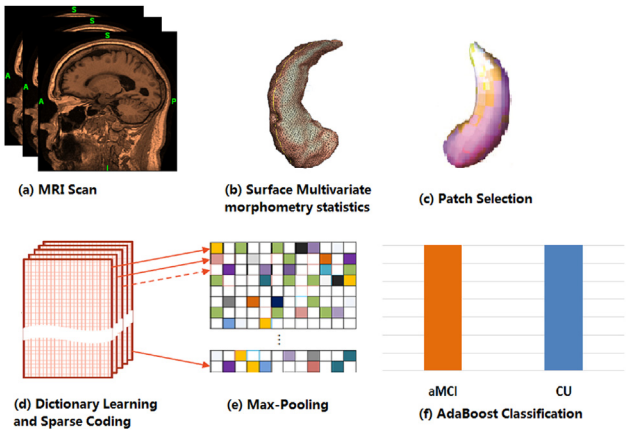

P3-285

PATCH-BASED SPARSE CODING AND MULTIVARIATE SURFACE MORPHOMETRY FOR PREDICTING AMNESTIC MILD COGNITIVE IMPAIRMENT AND ALZHEIMER'S DISEASE IN COGNITIVELY UNIMPAIRED INDIVIDUALS

Jie Zhang[1], Yalin Wang[1], Qingyang Li[1], Jie Shi[1], Robert Bauer, III[2], **Kewei Chen**[2], Eric M. Reiman[2], Richard J. Caselli[3], Cynthia M. Stonnington[3], *[1]Arizona State University, Tempe, AZ, USA; [2]Banner Alzheimer's Institute, Phoenix, AZ, USA; [3]Mayo Clinic Arizona, Scottsdale, AZ, USA. Contact e-mail: kewei.chen@bannerhealth.com*

Background: Neuroimaging biomarkers in combination with classification methods have shown promise as a tool for predicting progression to the clinical stage of Alzheimer's disease (AD). The hippocampus is affected in late preclinical and early clinical stages of AD. We previously described a method capable of detecting subtle changes in hippocampal surfaces, based on the surface fluid registration and multivariate tensor-based morphometry (mTBM) statistics. We now describe a method for distinguishing between cognitively unimpaired older adults who do or do not subsequently progress to amnestic Mild Cognitive Impairment (aMCI) using our new patch-based sparse-coding system with surface multivariate morphometry statistics (MMS) from the hippocampus. **Methods:** From the Arizona APOE cohort, a longitudinal study of cognitively unimpaired persons with two, one and no copies of the apolipoprotein E (APOE4) allele with a reported first degree family history of possible AD dementia, we examined volumetric MRI data from 18 cognitively unimpaired participants approximately 2 (1.8 ± 0.8) years before progression to the clinical diagnosis of aMCI and 35 participants who were matched for age and sex and remained unimpaired for $\geq$4 years. We segmented each individual MRI scan with FSL (http://fsl.fmrib.ox.ac.uk/fsl/fslwiki), parameterized the hippocampal surfaces as described previously, and generated the surface MMS consisting of mTBM and radial distance (RD). We constructed a collection of overlapping patches on the surface as the initial sparse coding dictionary. Stochastic Coordinate Coding was then applied to learn a dictionary and sparse codes. We used the max-pooling algorithm on the newly learned high-dimensional features to obtain a final set of low-dimensional features. Finally, an AdaBoost classifier was applied to categorize aMCI and cognitively unimpaired individuals with 5-fold leave-one-out cross validation adopted to evaluate classification accuracy, sensitivity, specificity, positive and negative predictive values. **Results:** The best prediction result of aMCI was achieved with our MMS features, with 96% accuracy, 100% sensitivity, 95% specificity, 86% positive and 100% negative predictive values. **Conclusions:** While our findings should be considered preliminary, sparse coding with the sensitivity of surface multivariate morphometry may be applied to volumetric MRIs to predict imminent progression from the preclinical to clinical stages of AD with great accuracy.

Table 1
Experiment Result of Hippocampal

Hippocampal	*RD*	*RD_left*	*RD_right*	*mTBM*	*mTBM_left*	*mTBM_right*	*MMS*	*MMS_left*	*MMS_right*
Accurcy	0.77	0.62	0.54	0.92	0.69	0.54	**0.96**	0.77	0.54
Sensitivity	1.00	0.33	0.20	0.75	0.60	0.25	**1.00**	0.50	0.33
Specificity	0.75	0.36	0.75	1.00	0.75	0.67	**0.95**	0.82	0.60
ppv	0.33	0.67	0.33	1.00	0.60	0.25	**0.86**	0.33	0.20
npv	1.00	0.60	0.60	0.90	0.75	0.67	**1.00**	0.90	0.75